Segregation of sedimenting grains of different densities in an oscillating velocity field of strongly nonlinear surface waves

A. B. Ezersky[1] and F. Marin[2]

[1]*Laboratoire Morphodynamique Continentale et Côtière, UMR CNRS 6143, Université de Caen-Basse Normandie/Université de Rouen, 2–4 rue des Tilleuls, 14000 Caen, France*

[2]*Laboratoire d'Ondes et Milieux Complexes, FRE CNRS 3102, Université du Havre, 25 rue P. Lebon, Boîte Postale 540, 76058 Le Havre cedex, France*

(Received 26 February 2008; published 8 August 2008)

This paper reports the results of an experimental and theoretical study of the segregation of heavy (sand) and light [polyvinyl chloride (PVC)] grains under the action of intense nonlinear water waves, solitons. The tests are carried out with initially carefully mixed grains at the bottom of a wave flume used in resonant mode. Ripples form on the bed and the segregation process is considered after the stopping of the wave paddle. The waves are damped and the PVC grains concentrate in a narrow region close to the ripple crest. A theoretical model explaining this grain density segregation is developed.

DOI: 10.1103/PhysRevE.78.022301 PACS number(s): 45.70.Mg, 45.70.Qj

I. INTRODUCTION

The formation of a rippled bottom profile under the action of linear or weakly nonlinear waves is well known in the literature [1–7]. The ripples significantly affect sediment transport, the dispersion of pollutants, and wave damping due to energy dissipation at the bed. The formation of these patterns has been considered in the cases of homogeneous [1–5] and heterogeneous [6,7] sediments disposing on the bottom. The authors of [6] considered the case of size-graded sediments; they have shown that when ripples are formed, the coarser sediments accumulate along the crests. Under the action of surface waves, grains of different sizes may form complex spatial patterns, like those visualized in [7]. It was found that grains that had been mixed were redistributed so that a volume stratification of the bottom occurred: grains of the same size were accumulated in layers of definite thickness.

In natural conditions waves may be highly nonlinear. It is well known that when an oscillatory wave moves into shoaling water, the wave amplitude becomes higher, the trough becomes flatter, and the surface profile approaches a solitary wave form before wave breaking occurs [8]. In other respects, long surface waves such as tsunamis often behave like solitary waves, highly nonlinear waves [9]. These waves may cause the suspension of particles. The formation of ripples for homogeneous sediments under solitons was studied in a wave flume used in resonant mode in [10]. However, grains with different physical characteristics are often found in the field. Organic materials at the bottom may be considered as grains whose density is less than the density of sand. In the present study, ripples are formed under solitons excited in the same way as in [10], with density-heterogeneous sediments, sand and polyvinyl chloride (PVC) grains. The aim of the present work is to study the grain segregation which takes place after the hydrodynamic forcing is stopped, when the water waves are damped and sedimentation of suspended particles occurs. A theoretical model is proposed to explain the experimental observations.

II. EXPERIMENTAL EVIDENCE OF GRAIN SEGREGATION

The tests have been carried out in a 10-m-long and 0.49-m-wide wave flume. The mean water depth was $D=0.26$ m. Surface waves are produced by an oscillating paddle at one end of the flume. An almost perfect reflection takes place at the other end of the flume. The frequency of the oscillating paddle is chosen to be very close to the resonant frequency $f_r=0.165$ Hz corresponding to the mode for which the wavelength is equal to the flume length. In this case, the wavelength L_h of the standing wave equals the effective flume length (9.63 m). The $D/L_h=0.027$ ratio lies in the range of the shallow water approximation. The present test conditions are chosen such that one soliton propagates in each direction of the flume over the time period of the flow; the shape of this soliton is well represented by the theoretical sech-squared profile η_S of solitons [11],

$$\eta_S = A_S \operatorname{sech}^2\left(\sqrt{\frac{3A_S}{4D^3}}(x - V_{\mathrm{sol}}t)\right), \tag{1}$$

where A_S is the soliton amplitude, x the distance measured in the horizontal direction, t the time, and V_{sol} the propagation velocity of the soliton: $V_{\mathrm{sol}}=V_0(1+A_S/2D)$, V_0 being the harmonic wave speed: $V_0=\sqrt{gD}$. The free surface displacement η is given by [11]

$$\eta(x,t) = \eta_S(x - V_{\mathrm{sol}}t) + \eta_S(x + V_{\mathrm{sol}}t) + 2A_0 \cos(kx)\sin(\omega t - \varphi_S), \tag{2}$$

where A_0 is the harmonic wave amplitude, $k=2\pi/L_h$ the wave number of the harmonic waves, and φ_S the phase shift between the soliton and the harmonic wave. For the present tests, we have $65<A_S<75$ mm and $A_0\approx 6$ mm. The corresponding value of the Reynolds number R_e defined using the velocity in the wave close to the bottom may be estimated as $R_e\approx 1.6\times 10^5$ [11]. Preliminary tests were carried out with a 20 mm sand layer at the bottom, without PVC grains. The sand is characterized by a median grain diameter $d_S=0.16$ mm and by a relative density $s=2.65$. For the other

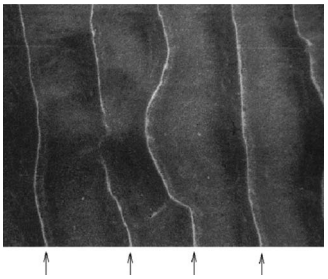

FIG. 1. Typical top view of the concentration of PVC grains on the ripple crests (marked by arrows) when the fluid motion has damped. The characteristic spatial period of sand ripples is 15 cm. The characteristic width of the region above the ripple crests where the PVC grains concentrate is 0.5–1 cm.

tests, 1 vol % PVC grains of relative density $s=1.35$ were added to the sand, in order to study the grain segregation induced by the solitons. For our experiments we have chosen PVC grains of two types: the first type (PVC1) is characterized by a median grain diameter $d_1=0.12$ mm, while the second type (PVC2) has a median grain diameter $d_2=0.20$ mm. Let us consider the Froude (Fr) and Stokes (St) numbers defined by $\mathrm{Fr}=U_b/\sqrt{[(\rho_{s,\mathrm{PVC}}/\rho_w)-1]gd_{s,\mathrm{PVC}}}$ and $\mathrm{St}=d_{s,\mathrm{PVC}}^2\rho_{s,\mathrm{PVC}}\omega/18\nu\rho_w$, where U_b is the amplitude of the flow velocity close to the bottom, ρ the density, ω the flow pulsation, ν the fluid kinematic viscosity, and the indices s, PVC, and w correspond to sand, PVC, and water, respectively. The value of Fr may be estimated to be 8 for the sand, 20 for the PVC1 grains, and 15 for the PVC2 grains. The Stokes number is a small parameter for the present tests: we have $\mathrm{St}=4\times10^{-3}$ for the sand, $\mathrm{St}=10^{-3}$ for the PVC1 grains, and $\mathrm{St}=3\times10^{-3}$ for the PVC2 grains.

The experiments were carried out as follows. Before each test, the sand (99 vol %) and the plastic PVC1 or PVC2 grains (1 vol %) were carefully mixed and the mixture was distributed uniformly over the bottom of the flume; the bed was initially flat for all the tests. Because of the small concentration of plastic grains they could hardly be seen on the bottom. We switched on the wave maker and a steady-state regime of soliton excitation was obtained after a few minutes. Ripples formed rapidly along the flume and a strong interaction occurred between the bed ripples and the nonlinear surface waves, as shown in [12]. The size and the shape of these ripples significantly change from one end of the flume to the other end, in the same way as for homogeneous sediments [10]. The wave maker was switched off when the steady state of the surface wave soliton—bed ripple system was reached. At this steady state, the characteristic ripple wavelength and height were 15 and 2.5 cm, respectively, in the area where the ripples were the biggest, that is, close to the nodes of the standing harmonic wave located at one-quarter and three-quarters of the flume length [10]. A short time later, the wave motions in the channel were damped; the characteristic time of surface wave decay was $T_d=1/\gamma\approx300$ s. As the wave motions were damping, we observed the appearance of regions where PVC grains accumulated. The grains were concentrated in a narrow region in the immediate vicinity of ripple crests (Fig. 1). Despite the small concentration of plastic grains in the PVC1-sand and PVC2-sand mixtures, this effect was excellently visualized because of the different colors of PVC and sand.

III. THEORETICAL MODEL

In this section we present a physical mechanism leading to a PVC grain concentration in the neighborhood of sand ripple crests. We describe the grains as a continuum with a volume fraction $C_{s,\mathrm{PVC}}(x,y,t)=\pi d_{s,\mathrm{PVC}}^3 n_{s,\mathrm{PVC}}/6$, where n is the number of grains per unit volume and d the grain diameter.

A. Equations describing the motion of grains

We use the following equations to describe sedimenting particles:

$$\rho_{s,\mathrm{PVC}}\frac{\pi d_{s,\mathrm{PVC}}^3}{6}\frac{d\vec{V}_{s,\mathrm{PVC}}}{dt}=3\pi\rho_w\nu d(\vec{U}-\vec{V})-\vec{\nabla}p+(\rho_{s,\mathrm{PVC}}-\rho_w)\frac{\pi d_{s,\mathrm{PVC}}^3}{6}\vec{g}, \quad (3)$$

$$\frac{\partial C_{s,\mathrm{PVC}}}{\partial t}+\vec{\nabla}\cdot C_{s,\mathrm{PVC}}\vec{V}_{s,\mathrm{PVC}}=0, \quad (4)$$

where $\vec{V}$ is the velocity of grains, $\vec{g}$ is the acceleration due to gravity, ν is the fluid kinematic viscosity, $\vec{U}$ is the flow velocity vector, and p is the pressure in the fluid. It should be mentioned that we take into account only the Stokes force and do not consider the turbulent drag. It is supposed that after the wave maker is stopped, turbulence decays much more rapidly than the waves. Let us calculate the pressure gradient, assuming that it is possible to replace solid grains by liquid grains:

$$\rho_w\frac{d\vec{U}}{dt}=-\vec{\nabla}p. \quad (5)$$

We neglect here the viscosity terms because we are going to consider a flow field with components $U_x, U_y\propto x+\beta y$, and in this case the viscosity terms $(\partial^2/\partial x^2+\partial^2/\partial y^2)(\vec{U})$ vanish. Substituting Eqs. (5) into Eq. (4) we get after some transformation

$$\vec{V}+\frac{\mathrm{St}}{\omega}\frac{d\vec{V}}{dt}=\vec{U}+\frac{\mathrm{St}}{\omega}\frac{\rho_w}{\rho_{s,\mathrm{PVS}}}\frac{d\vec{U}}{dt}+\frac{(\rho_{s,\mathrm{PVS}}-\rho_w)}{\rho_w}\vec{g}. \quad (6)$$

Note that the velocity of the flow $\vec{U}$ is considered to change periodically in time with the pulsation ω. For our experimental conditions the Stokes number St is a small parameter: $\mathrm{St}\sim10^{-3}$ (Sec. II). The grain velocity $\vec{V}$ does not coincide with the flow velocity $\vec{U}$. It is possible to use St as an expansion parameter and write the grain velocity as (see [13])

$$\vec{V}=\vec{V}^{(0)}+\mathrm{St}\,\vec{V}^{(1)}+\mathrm{St}^2\vec{V}^{(2)}+\cdots. \quad (7)$$

From Eqs. (6) and (7) we can obtain a solution in the form

$$\vec{V}^{(0)} = \vec{U} - \vec{e}_y \frac{d_{s,\mathrm{PVC}}^2(\rho_{s,\mathrm{PVC}} - \rho_w)}{18\nu\rho_w} g \equiv \vec{U} - \vec{e}_y U_0,$$

$$\vec{V}^{(1)} = -\frac{1}{\omega}\left(\frac{d(\sigma\vec{U} - \vec{e}_y U_0)}{dt}\right). \tag{8}$$

In Eq. (8) $U_0 = d_{s,\mathrm{PVC}}^2(\rho_{s,\mathrm{PVC}} - \rho_w)g/18\nu\rho_w$ is the Stokes sedimentation velocity, and $\sigma = 1 - \rho_w/\rho_{s,\mathrm{PVC}}$. The velocity U_0 depends on the type of grain but does not depend on time and spatial coordinates. We restrict ourselves to the first approximation. The terms of second and higher degrees have been analyzed in [13].

B. Model of flow with hyperbolic point

We consider a very simple model assuming in the first approximation that the bottom is flat. Using experimental data we model this flow in the neighborhood of each sand crest by the stream function $\psi = -a(\alpha x + y)y$. The coefficient α is a nondimensional constant and a has the dimension of an angular frequency. We will consider a half plane $y > 0$; the point $x=0$, $y=0$ corresponds to the region above the crest of sand ripples. We assume that slip conditions occur on the surface $y=0$. For the velocity field, we have

$$U_x = \frac{\partial\psi}{\partial y} = -a(\alpha x + 2y), \quad U_y = -\frac{\partial\psi}{\partial x} = a\alpha y. \tag{9}$$

The direction of the flow changes periodically in time, whereas the position of the hyperbolic point remains stationary. In the present theoretical model the bottom is assumed to be plane, whereas in real conditions it has a rippled profile. We will neglect this discrepancy for the investigation of the grains motion near the hyperbolic point. In our experiments the characteristic scale of ripples is $\lambda = 15$ cm. Near the ripple crest it is possible to consider a small region with a characteristic scale $\ell = 1$ cm as a plane. Our approximation is valid in the first order of the parameter $\ell/\lambda \ll 1$.

It should also be emphasized that our model supposes slip conditions for $y=0$. In fact, we deal with oscillation in viscous fluid. Near the sand bottom there is an oscillating boundary layer of thickness $\delta = \sqrt{\nu/2\omega} \approx 0.07$ cm. We suppose that this thickness is much less than the other characteristic scales of motion in the vicinity of the hyperbolic point, and that outside this layer it is possible to neglect the influence of viscosity.

Let us consider $\alpha = \alpha_0 \sin(\omega t)$, $a = a_0 \sin(\omega t)$. The sequence of pictures of the corresponding velocity field is shown in Fig. 2. The parameter α_0 controls the maximal slope of the line separating the forward and return flows.

As $\alpha_0 \to 0$, the sector enclosing a return flow is reduced to zero. With time increasing from $\omega t = 0$ (for $\omega t = 0$, $\vec{U} = \vec{0}$), a hyperbolic point located at $x=0$, $y=0$ arises; the region of return flow for $x<0$ expands and its maximum size is reached when $\omega t = \pi/2$. At $\omega t = \pi$, the velocity direction changes and the region with the return flow appears for $x > 0$. For the vorticity $\vec{\Omega}$, we get

$$\vec{\Omega} = \vec{\nabla} \times \vec{U} = 2a\vec{e}_z. \tag{10}$$

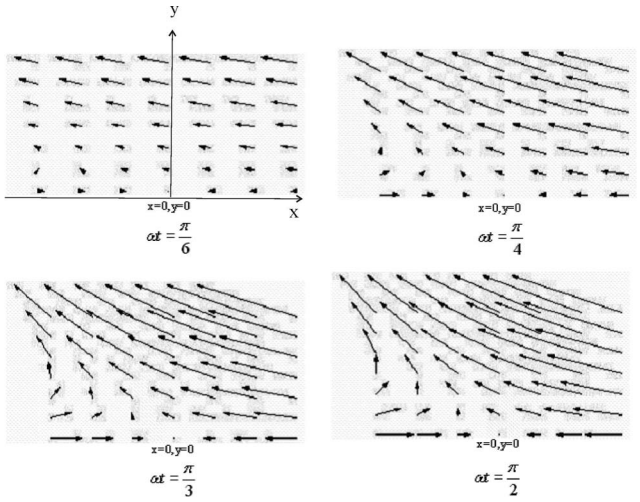

FIG. 2. Velocity fields $\vec{U} = (U_x, U_y)$ in the (x,y) plane for different times $\omega t = \pi/6, \pi/4, \pi/3, \pi/2$ obtained from Eq. (10) for $\alpha_0 = 2$. For our flow model, the velocity field is identical for $\omega t = \pi/6$ and $\omega t = \pi - \pi/6 = 5\pi/6$, etc. For $\omega t = \pi/6$ and $\omega t = \pi + \pi/6 = 7\pi/6$, etc., the horizontal component of velocity field changes sign: $U_x(x) \to -U_x(-x)$.

According to our model the flow has a spatially homogeneous vorticity [Eq. (10)] varying periodically in time. It should be mentioned that, according to the theoretical model, the flow has spatially homogeneous vorticity. In fact, we use the theoretical model in a narrow region near the crest. Outside this narrow region the model is not applicable. Our consideration concerns only a small region near the hyperbolic point.

We note that the evolution of the vorticity field appearing as a result of the interaction of surface waves with a rippled bottom profile was investigated experimentally in [14]. It was found that in the vicinity of ripple crests, regions with high values of the vorticity were generated. Flows with streamlines in the vicinity of crests topologically equivalent to those presented in Fig. 2 have been discussed in a large number of papers (see, for example, [1]). The most interesting feature for grain motion is the appearance of a hyperbolic point positioned at $x=0$, $y=0$. Grains of sand and PVC participate in two different types of motion: they sediment and oscillate because they are drawn by an oscillating velocity field $\vec{U}$.

C. Evolution of particle concentration near the hyperbolic flow

Neglecting the terms proportional to St^2 in the expansion (7), we substitute the expressions (8) into the equation of motion (6). For the components of the grain velocity field V_x, V_y near the sand ripple we obtain the following expressions [the indices s, PVC have been omitted; Eqs. (9) for the components U_x, U_y have been used]:

$$V_x = -\sigma a(\alpha x + 2y) + \frac{\mathrm{St}}{\omega}[\sigma(\dot{a}\alpha + a\dot{\alpha})x + \dot{a}y - \sigma^2 a^2 \alpha^2 x - 2\sigma a U_0], \tag{11}$$

$$V_y = \sigma a \alpha y - U_0 - \frac{\mathrm{St}}{\omega}[\sigma(\dot{a}\alpha + a\dot{\alpha})y + \sigma^2 a^2 \alpha^2 y - \sigma a \alpha U_0]. \tag{12}$$

After the substitution of the expressions for V_x and V_y into Eq. (5), and supposing that the concentration of particles does not depend on spatial coordinates x and y, which is obtained for the initial condition $C(t=0)=C_0$, we get

$$\dot{C} = \frac{\mathrm{St}}{\omega}(2\sigma^2 a^2 \alpha^2) C. \tag{13}$$

It must be noted that the concentration evolution does not depend on the fall velocity. We suppose that the change of the concentration during the wave period is small compared with the grains concentration. It is in good agreement with the experimental data since segregation takes place during several dozens of period. This explains that it is possible to average Eq. (13) over the time $t=1/\omega$ and to obtain a differential equation for the quantity $\langle C \rangle$:

$$\langle \dot{C} \rangle = 2\frac{\mathrm{St}}{\omega}\langle(\sigma^2 a^2 \alpha^2)\rangle \langle C \rangle. \tag{14}$$

The segregation of grains was observed during the decay of surface waves. It is reasonable to consider that the vorticity decays in the same way as the amplitude of the surface wave:

$$\langle \alpha^2 a^2 \rangle = \langle \alpha_0^2 a_0^2 e^{-2\gamma t} \sin^4 \omega t \rangle = \tfrac{1}{4}\alpha_0^2 a_0^2 e^{-2\gamma t}. \tag{15}$$

In Eq. (15), a_0 is half of the amplitude of the vorticity before the wave maker is stopped and γ is the rate of exponential decay of the surface waves. It is easy to integrate Eq. (14) and to obtain the temporal evolution of the concentration $\langle C \rangle$ near the hyperbolic point:

$$\langle C \rangle = \langle C_0 \rangle \exp\left(\frac{\mathrm{St}}{4\omega\gamma}\sigma^2 a_0^2 \alpha_0^2 [1 - \exp(-2\gamma t)]\right), \tag{16}$$

where $\langle C_0 \rangle$ is the value of $\langle C \rangle$ at $t=0$. The concentration of particles grows for $\gamma t \ll 1$ as $\langle C \rangle \propto 1+2\gamma t$ and tends toward the constant value $\langle C \rangle = \langle C_0 \rangle \exp[(\mathrm{St}/4\omega\gamma)\sigma^2 a_0^2 \alpha_0^2]$ for $\gamma t \gg 1$.

To understand qualitatively why the concentration growths in the vicinity of the hyperbolic point, it is possible to calculate the averaged velocity of particles $\langle V_x \rangle$ and $\langle V_y \rangle$. Using Eqs. (11) and (12) we have

$$\langle V_x \rangle = -x\left(\frac{\sigma}{2} a_0 \alpha_0 e^{-\gamma t} + \frac{\mathrm{St}}{4\omega} a_0^2 \alpha_0^2 e^{-2\gamma t}\right),$$

$$\langle V_y \rangle = -(U_0 - y\sigma a_0 \alpha_0 e^{-\gamma t})\left(1 - \frac{\mathrm{St}}{\omega}\sigma a_0 \alpha_0 e^{-\gamma t}\right). \tag{17}$$

The averaged horizontal velocity of particles according to Eq. (17) is negative ($\langle V_x \rangle < 0$) for $x>0$ and positive ($\langle V_x \rangle > 0$) for $x<0$. It means that all particles are moving toward $x=0$ (toward the hyperbolic point) during the wave decay. Also all particles sink $\langle V_y \rangle < 0$ for small values of the amplitude of the velocity field (large enough value of γt).

Our simple model shows that the grain concentration grows in the vicinity of the hyperbolic point with increasing values of the time. The characteristic time of this process equals the time of surface wave decay, $T_d = 1/\gamma$. It should be emphasized that the increase of the concentration of sand and PVC grains occurs in different ways. Indeed, let us estimate the sedimentation times. Due to turbulence the grains were suspended in a layer approximately $D_l \sim 20$ cm thick. The time necessary for the suspended grains to reach the bottom after the wave maker was stopped may be estimated to be $\tau_s \approx D_1/U_{0s} = 18 D_1 \nu \rho_w / d_s^2 (\rho_s - \rho_w) g \approx 9$ s for the sand, $\tau_{\mathrm{PVC1}} \approx 70$ s for the PVC1 grains, and $\tau_{\mathrm{PVC2}} \approx 30$ s for the PVC2 grains. The concentration of the PVC grains should consequently increase everywhere at the bed surface; however, the PVC grains are observed only close to the ripple crests when the waves have damped. The segregation mechanism may be explained as follows. After the wave maker has been stopped and for $t < \tau_s$, both sand and PVC grains are concentrated near the ripple crests. For $t > \tau_s$, when most sand grains have settled on the bottom, only PVC grains begin to concentrate near the crests. It is possible to estimate the increase in PVC grain concentration using Eq. (17) with $t = \tau_{\mathrm{PVC1,2}}$. For the present experimental conditions, we have $\omega \approx 1$ rad/s, $\sigma \approx 0.25$, and $\alpha_0 \approx 1$. We did not measure the parameter a_0 as special equipment is demanded for that. Such a measurement was carried out above an artificial rippled bed in the paper [14]. According to this paper, the characteristic value of the vorticity Ω near the ripples crests may be estimated to be in the range $20(U_x/\lambda) < \Omega < 30(U_x/\lambda)$, where U_x is the characteristic value of the horizontal flow velocity. In our experiments, the value of U_x just after the excitation of solitons is stopped is approximately 40 cm/s, and $\lambda = 15$ cm. Using these values, we get $3 < \langle C \rangle / \langle C_0 \rangle < 20$ for the PVC1 grains and $6 < \langle C \rangle / \langle C_0 \rangle < 55$ for the PVC2 grains. This explains why the PVC grains (PVC1 and PVC2), characterized by a lower density than that for the sand grains, concentrate close to the ripple crests, at the end of the surface wave decay.

[1] R. A. Bagnold, Proc. R. Soc. London, Ser. A **187**, 1 (1946).
[2] P. Nielsen, J. Geophys. Res. **86**, 6467 (1981).
[3] P. Blondeaux, J. Fluid Mech. **218**, 1 (1990).
[4] G. Vittori and P. Blondeaux, J. Fluid Mech. **218**, 19 (1990).
[5] A. Stegner and J. E. Wesfreid, Phys. Rev. E **60**, R3487 (1999).
[6] E. Foti and P. Blondeaux, Coastal Eng. **25**, 237 (1995).
[7] G. Rousseaux, H. Caps, and J.-E. Wesfreid, Eur. Phys. J. E **13**, 213 (2004).
[8] W. H. Munk, Ann. N.Y. Acad. Sci. **51**, 376 (1949).
[9] P. L.-F. Liu, C. E. Synolakis, and H. H. Yeh, J. Fluid Mech. **229**, 675 (1991).
[10] F. Marin and A. B. Ezersky, Eur. J. Mech. B/Fluids **27**, 3 (2008).
[11] A. Ezersky, O. Poloukhina, J. Brossard, F. Marin, and I. Mutabazi, Phys. Fluids **18**, 067104 (2006).
[12] F. Marin, N. Abcha, J. Brossard, and A. B. Ezersky, J. Geophys. Res. **110**, F04S17 (2005).
[13] A. Druzhinin, J. Fluid Mech. **297**, 49 (1995).
[14] F. Marin, Coastal Eng. **50**, 139 (2004).